Our data suggest that the amount of CD8β expressed is also critical for positive selection. One possible explanation for the role of CD8β is that CD8αβ may bind to class I MHC molecules with higher affinity than that of CD8αα, and only CD8αβ-MHC interaction is sufficient for positive selection. Because positive selection probably requires a relatively weak interaction between the TCR and the peptide-MHC complex (stronger interactions result in clonal deletion), it may be far more sensitive to the relative contribution of the CD8 coreceptor than when studied in in vitro functional assay systems.

In independent studies, we showed that the lack of the CD8α cytoplasmic domain resulted in a dramatically decreased efficiency in positive selection, arguing that not only binding to class I MHC α3 domain but also signaling through the CD8α cytoplasmic region are required for positive selection (*22*). Surprisingly, $p56^{lck}$, which binds to the cytoplasmic domain of CD4 or CD8α, is not necessary for positive and negative selection (*23*). As for the role of the cytoplasmic region of CD8β, it is short and there is no motif for the binding of any known signaling molecules (*24*). In addition, experiments in hybridoma systems have suggested that only extracellular but not the cytoplasmic portion of CD8β is critical for the augmentation of interleukin-2 release (*7*). Taken together, it is unlikely that CD8β contributes to positive selection by signaling through its cytoplasmic region. We thus favor the hypothesis that the significant difference between CD8αβ and CD8αα molecules lies in their extracellular domains. The mice generated in this study should be useful in elucidating the molecular requirements for positive selection in the CD8 lineage.

REFERENCES AND NOTES

1. S. L. Swain, *Immunol. Rev.* **74**, 129 (1983); D. R. Littman, *Annu. Rev. Immunol.* **5**, 561 (1987).
2. M.-L. Blue, K. A. Craig, P. Anderson, K. Branton, S. F. Schlossman, *Cell* **54**, 413 (1988); A. Norment, R. D. Salter, P. Parham, V. H. Englehard, D. R. Littman, *Nature* **336**, 79 (1988); J. M. Connolly, T. A. Potter, E.-M. Wormstall, T. H. Hansen, *J. Exp. Med.* **168**, 325 (1988); T. A. Potter, T. V. Rajan, R. F. Dick II, J. A. Bluestone, *Nature* **337**, 73 (1989); R. D. Salter *et al.*, *ibid.* **338**, 345 (1989); R. D. Salter *et al.*, *ibid.* **345**, 41 (1990).
3. A. Norment and D. R. Littman, *EMBO J.* **7**, 3433 (1988).
4. J. R. Parnes, *Adv. Immunol.* **44**, 265 (1989).
5. N. Torres-Nagel *et al.*, *Eur. J. Immunol.* **22**, 2841 (1992).
6. J. Gabert *et al.*, *Cell* **50**, 545 (1987); Z. Dembic *et al.*, *Nature* **326**, 510 (1987).
7. C. J. Wheeler, P. von Hoegen, J. R. Parnes, *Nature* **357**, 247 (1992); F. Letourneur *et al.*, *Proc. Natl. Acad. Sci. U.S.A.* **87**, 2339 (1990); S. Karaki, M. Tanabe, H. Nakauchi, M. Takiguchi, *J. Immunol.* **149**, 1613 (1992).
8. K.-i. Nakayama *et al.*, *Science* **261**, 1584 (1993).
9. K.-i. Nakayama, Y. Shinkai, K. Okumura, H. Nakauchi, *J. Immunol.* **142**, 2540 (1989).
10. K.-i. Nakayama *et al.*, *ibid.* **148**, 1919 (1992); K.-i. Nakayama and H. Nakauchi, *Int. Immunol.* **5**, 419 (1993).
11. Cloned genomic DNA corresponding to the *CD8β* locus was isolated from a library of strain B10.A mouse DNA as described (*9*). The targeting vectors, p8βKO-NEO and p8βKO-HYG, were constructed by a replacement of a 0.9-kb Sca I–Pst I fragment containing most of the CD8β immunoglobulin-like domain (*9*) with either a PGK-neo-polyadenylate [poly(A)] cassette derived from pKJ-1 (*25*) or a PGK-hyg-poly(A) cassette [H. te Riele, E. R. Maandag, A. Clarke, M. Hooper, A. Berns, *Nature* **348**, 649 (1990)]. The targeting vectors contained 1.3 kb of homology 5′ and 6.0 kb 3′ of the drug resistance marker. The PGK-tk-poly(A) cassette (*25*) was ligated into a restriction site in a vector polylinker at the 3′ end of the insert. Maintenance, transfection, selection, and injection of ES cells were carried out as described elsewhere (*8*). Frequency of the homologous recombinations was 25.5% with p8βKO-NEO after first-round transfection and 18.8% with p8βKO-HYG after second-round transfection.
12. Lymph node cells and thymocytes (5×10^5) were prepared from control and knockout chimeras and stained with fluorescein isothiocyanate (FITC)–conjugated antibody to Ly-9.1, phycoerythrin (PE)–conjugated antibody to CD8β or PE-conjugated antibody to CD4, and biotinylated antibody to CD8α (PharMingen). Biotin conjugates were revealed by Red 613–streptavidin (GibcoBRL). The expression of CD8β (Fig. 3B) was analyzed with Ly-9.1–FITC, CD8β-PE, and TCRαβ-biotin (PharMingen) by gating on Ly-9.1^+TCR$\alpha\beta^+$ cells. Dead cells were excluded by staining with propidium iodide (Boehringer Mannheim). Flow cytometric analysis was done by FACScan (Becton Dickinson).
13. K.-i. Nakayama, A. Sarai, H. Nakauchi, *Immunogenetics* **33**, 206 (1991); D. Blanc *et al.*, *Eur. J. Immunol.* **18**, 613 (1988); S. D. Gorman, Y. H. Sun, R. Zamoyska, J. R. Parnes, *J. Immunol.* **140**, 3646 (1988).
14. K.-i. Nakayama and D. Y. Loh, unpublished observations.
15. T. Lin, G. Matsuzaki, H. Kenai, T. Nakamura, K. Nomoto, *Eur. J. Immunol.* **23**, 1968 (1993).
16. A 16.5-kb genomic DNA fragment, containing the whole *CD8β* gene (*9*) ligated to a puromycin-resistant gene driven by the PGK promoter, was transfected by electroporation into $CD8\beta^{-/-}$ ES cells (EEH603) and selected by puromycin-containing medium (1.0 μg/ml). We injected clones carrying the transfected *CD8β* gene into C57BL/6 blastocysts, generating chimeric mice.
17. D. Y. Loh, *New Biol.* **3**, 924 (1991).
18. W. C. Sha *et al.*, *Proc. Natl. Acad. Sci. U.S.A.* **87**, 6186 (1990).
19. W.-P. Fung-Leung *et al.*, *Eur. J. Immunol.* **23**, 212 (1993).
20. L. A. Sherman, S. V. Hesse, M. J. Irwin, D. La Face, P. Peterson, *Science* **258**, 815 (1992).
21. E. A. Robey *et al.*, *Cell* **69**, 1089 (1992); N. A. Lee, D. Y. Loh, E. Lacy, *J. Exp. Med.* **175**, 1013 (1992).
22. W.-P. Fung-Leung *et al.*, *Eur. J. Immunol.* **23**, 2834 (1993).
23. K.-i. Nakayama and D. Y. Loh, *Science* **257**, 94 (1992); I. T. Chan *et al.*, *ibid.* **261**, 1581 (1993).
24. H. Nakauchi, Y. Shinkai, K. Okumura, *Proc. Natl. Acad. Sci. U.S.A.* **84**, 4210 (1987).
25. V. L. Tybulewicz, C. E. Crawford, P. K. Jackson, R. T. Bronson, R. C. Mulligan, *Cell* **65**, 1153 (1991).

26. We thank P. Mombaerts, E. George, and R. Hynes for ES cell lines; A. Berns for the PGK-hyg-poly(A) cassette; P. Laird and R. Jaenisch for the PGK-puro-poly(A) cassette; Y. Shinkai for helpful discussions; and S. Kim and Q. Zhang for technical assistance. Supported by the Howard Hughes Medical Institute (D.Y.L.) and NIH grant AI 34580 (D.Y.L.).

29 October 1993; accepted 6 January 1994

Persistence of Transients in Spatially Structured Ecological Models

Alan Hastings* and Kevin Higgins

Simple discrete-time ecological models for a species with alternating reproduction and dispersal are shown to have complex transient dynamics. If the density dependence (nonlinearity) is strong enough, then the time required to reach the final dynamics is usually very long, approaching thousands of generations, and there are typically very sudden changes in the form of the dynamics. Apparent chaos can change to cycles or vice versa. These results are consistent with observed sudden changes in the form of the dynamics of a single species and imply that transient dynamics of ecological models may be more relevant than long-term behavior.

Ecological theory has typically been based on analysis of the long-term behavior of ecological models, with stability analysis as the primary tool (*1*, *2*). Even studies of nonequilibrium behavior, such as limit cycles or chaos, have focused on long-term behavior (*3*). We show that the long-term behavior of a simple ecological model for a species distributed along a one-dimensional habitat can be essentially irrelevant to the understanding of natural ecological systems because the form of the dynamics changes over long time scales. The model we use, in which juveniles (pelagic larvae) are redistributed along the coast each generation, has transient dynamics that are much longer than the time scale of significant environmental perturbations. Moreover, the transient dynamics can appear to be the final behavior, either chaotic or cyclic, and then the system can quickly change its dynamics without any underlying change in parameters.

These considerations have particular relevance when one is trying to understand

Division of Environmental Studies, Institute of Theoretical Dynamics, and Center for Population Biology, University of California, Davis, CA 95616, USA.

*To whom correspondence should be addressed.

the highly irregular dynamics of some species with pelagic larvae, such as sea urchins (*4–6*) and Dungeness crab (*7, 8*). More generally, long transients may play a major role in the "paradox of the plankton" (*9*) or outbreaks of insects (*10*). Different possible dynamic outcomes for the same parameters, multiple attractors, are a further complication (*11, 12*).

We used a simple model that retains the most important biological features of intertidal or subtidal organisms with pelagic larvae—density-dependent production of larvae, followed by redistribution along the coast, centered at the point of release. We ignored survivorship of adults from year to year (unless adult survivorship is high, our qualitative results do not change), which led to a model similar to one studied by Kot and Schaffer (*13*), who focused on asymptotic behavior.

The numerical scheme we used to study this model treats space as discrete blocks, leading to a system that is similar to a coupled map lattice (*14*) with global coupling. Our goal was to emphasize important ecological conclusions expected from previous results on long transients (*15, 16*) from coupled map lattice models with coupling only between adjacent cells. Coupled map lattices also have been used to study complex ecological models (*11, 17*) with local coupling. Our work emphasizes the importance of long transients within the context of ecologically more realistic dispersal regimes.

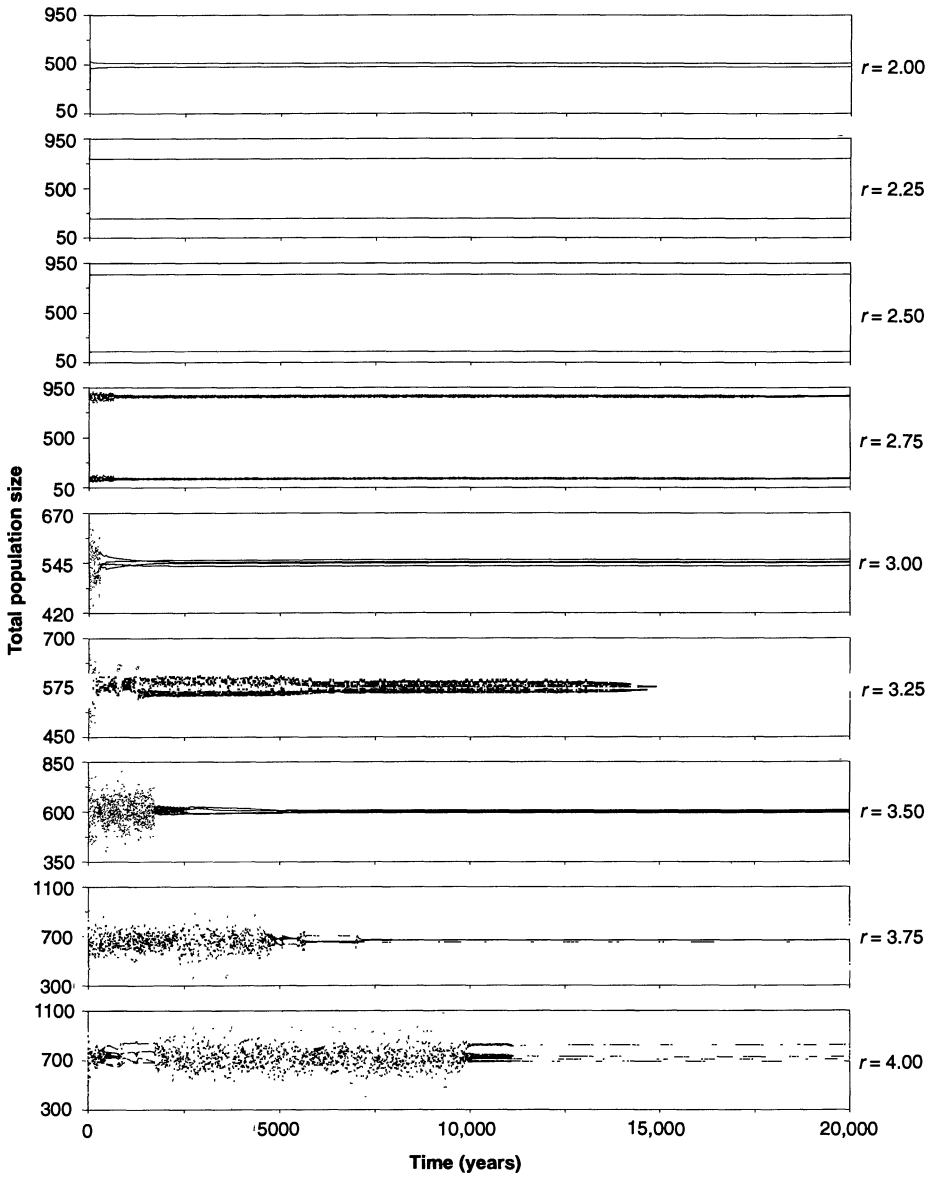

Fig. 1. Dynamics of a spatially structured model (*1–3*) of a population with pelagic larvae along a coastline as a function of the growth rate r. In all cases, the initial conditions were chosen randomly in space from a uniform distribution, and $D = 800$. The presence of long transients is apparent from the plots for all values of $r \geq 3.25$.

We assume that there is a finite length L of favorable habitat along the coast, denoting position along the coast by x, where $0 < x < L$. The number of larvae produced at position x in year t, $l(t,x)$, is given by the Ricker (*18*) formulation

$$l(t,x) = N(t,x)e^{r[1-N(t,x)]} \quad (1)$$

where we have scaled population size $N(t,x)$ so 1 is the equilibrium without spatial structure and r is the growth rate. Our results do not depend critically on our choice of the Ricker equation to describe density-dependent recruitment (*19*). Dispersal follows reproduction, so that the number of individuals at the location x is given by a summation of larvae released around the position x

$$N(t+1,x) = \int_0^L l(t,y)g(y,x)dy \quad (2)$$

where the probability that a larva released at y settles at x is given by the Gaussian

$$g(y,x) = \frac{e^{-D(y-x)^2}}{\sqrt{\pi/D}} \quad (3)$$

Here, D is a parameter measuring the dispersal distance, chosen to reflect parameter values determined from a two-dimensional model of larval transport (*8*). The choice of D does not critically affect our results (*20*), as our examples below show. In our model, the effective growth rate varies over space because larvae that disperse outside the region of interest are lost.

The time scale of ecological interest is tens or hundreds of years. However, analyses of other models analogous to those in (*1–3*) have typically focused on long-term dynamic behavior. We show that long-term dynamics do not predict the dynamics on a relatively short ecological time scale.

Although the analysis given here is not complete, our numerical studies show behavior of surprising complexity and variety. First, if the growth rate r is small enough, an equilibrium is approached (Fig. 1). Second, for higher growth rates, cyclic and chaotic behavior are possible (*21*). Third, if the growth rate is high enough, there can be long transients and then different stable asymptotic dynamics for the same growth rates, depending on initial conditions. Long transients are typical for values of $r \geq 3.25$ (Fig. 1).

To identify dynamic behavior visually, we plotted the total population size at time t, $\int_0^L N(t,x)dx$, versus the total population size at time $t - 1$. An equilibrium consists of a single point, cyclic behavior corresponds to a finite number of points, and quasi-cyclic behavior corresponds to points lying on a curve. Chaotic behavior would

lead to a more complex geometrical object.

Some of the wild possibilities are illustrated in Fig. 2. Starting from random initial conditions, there is little apparent form to the dynamics for almost 1000 years. Then, for almost 10,000 years the dynamics are usually cyclic, with several intervals (of up to 100 years) where the dynamics are very different. Finally, after 16,000 years the dynamics become chaotic.

This kind of unpredictable dynamics, with apparent changes from cycles to chaos or vice versa, is typical. Further examples are illustrated for several choices of r and for D (Fig. 3). We first focused on a moderate time scale of 100 to 200 years, recognizing that even this time scale may be much longer than the time scale of ecological interest. After 100 to 200 years, the dynamics have not even begun to settle down [Fig. 3, column (i)]: The patterns do not correspond to any of the potential long-term asymptotic behaviors. Local (in space) behavior is no more predictable.

We next examined the behavior of the model on a time scale of 1000 to 2500 years. The dynamic behavior shows indications of equilibrium, cyclic, or chaotic dynamics, depending on the parameters or initial conditions [Fig. 3, column (ii)]. However, the suggestion that the system has reached its asymptotic dynamics on this time scale is typically not correct (*15*, *16*). The dynamics on a time scale of 10,000 to 12,000 years could be different from the dynamics on a time scale of 1000 to 2500 years, changing from apparent chaos to cycles or vice versa [Fig. 3, column (iii)]. For other parameter choices, these changes in dynamics can take place on a shorter, ecological time scale.

Thus, after a major disturbance, population dynamics may be quite unpredictable for a long time. Continual disturbance may prevent the system from ever attaining one of the simple asymptotic behaviors. In other studies motivated by physical problems, the time scale for coupled lattice models to approach their asymptotic behavior has been observed to scale with the exponential (*16*) of the number of cells, or be even longer (*15*), indicating the extremely long transient behavior that is possible. Chaos acts as a noise amplifier, which, in combination with spatial structure, leads to extremely long transients.

In spatially structured systems, ecological time scales do not in general correspond to asymptotic behavior. Consequently, we expect "unpredictable" behavior for these systems, with "unexplained" changes in dynamics, as observed for sea urchins (*4*–*6*), Dungeness crab (*7*, *8*), plankton (*9*), and insects (*10*), for example. Thus, analyses should emphasize transient behavior as well as asymptotic behavior, particularly for disturbed systems. In the case of sea urchin

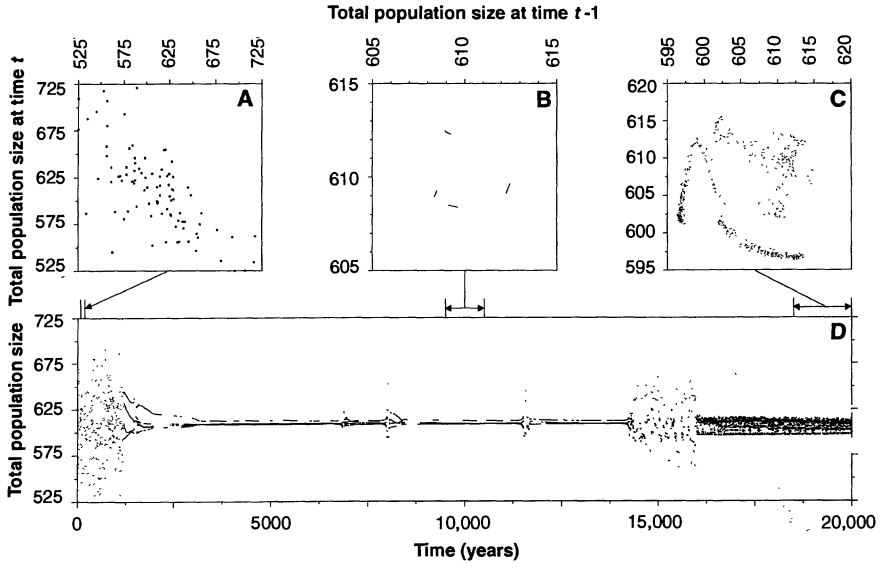

Fig. 2. Dynamics of a spatially structured model (*1*–*3*) of a population with pelagic larvae along a coastline at different time scales, for $r = 3.5$ and $D = 4000$. Plots of the population size at year t versus the population size at year $t - 1$ illustrate (**A**) no apparent pattern at the short time scale, (**B**) apparent quasi-cycles at the intermediate time scale, and (**C**) apparent chaos at the longest time scale. (**D**) The complete time series.

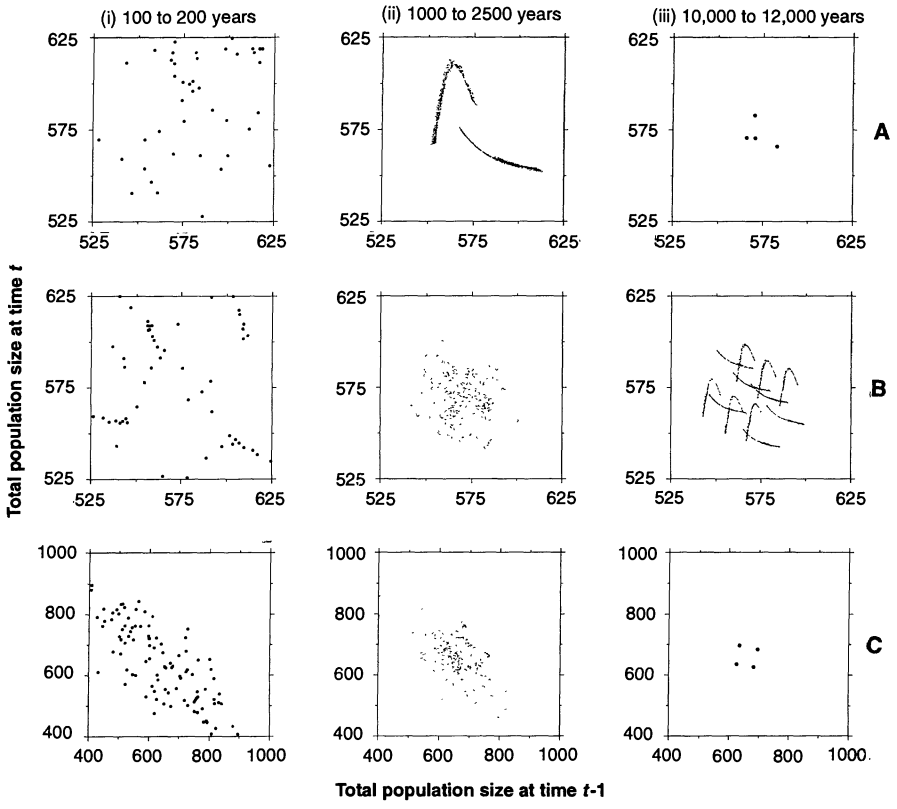

Fig. 3. Dynamics of a spatially structured model (*1*–*3*) of a population with pelagic larvae along a coastline for various time scales, initial conditions, and parameter values. The presence of long transients is apparent from the plots. The plots are of total population size at year t versus total population size at year $t - 1$, with each column representing different time scales and each row a different example. In row A, the habitat was divided into four segments of equal length, which were initially set at two different population levels, $r = 3.25$ and $D = 800$; the dynamics changed from an apparent chaos to a simple four-point cycle. In row B, the initial conditions were random in space, $r = 3.25$ and $D = 800$; the dynamics took a long time to approach a chaotic attractor. In row C, the initial conditions were random in space, $r = 3.75$ and $D = 400$; the dynamics took a long time to approach a simple four-point cycle. In all of these examples, the form of the dynamics from time scale (iii) $t = 10,000$ to 12,000 was still found at $t = 100,000$.

population eruptions in the northwestern Atlantic, there were great difficulties in finding an underlying cause (5). We have added the possibility of another "cause," namely, that population eruptions may be an underlying feature of the dynamics without any change in physical or biological conditions.

Efforts to detect density dependence are likely to fail precisely for those species with strong density-dependent recruitment (*22–24*) if they are spatially distributed in the fashion we have examined here. We have shown that long transient behavior is more likely to result when local density dependence is strong rather than weak. Thus, ironically, problems in detection of density dependence are most likely to occur for those species for which the underlying density-dependent mechanisms are in fact the strongest. Just this effect has been observed in studies of the viburnum whitefly (*24*).

REFERENCES AND NOTES

1. R. M. May, *Stability and Complexity in Model Ecosystems* (Princeton Univ. Press, Princeton, NJ, 1973).
2. J. Roughgarden, R. M. May, S. A. Levin, Eds., *Perspectives in Ecological Theory* (Princeton Univ. Press, Princeton, NJ, 1989).
3. A. Hastings, C. L. Hom, S. Ellner, P. Turchin, H. C. J. Godfray, *Annu. Rev. Ecol. Syst.* **24**, 1 (1993).
4. J. A. Estes, D. O. Duggins, G. B. Rathbun, *Conserv. Biol.* **3**, 252 (1989).
5. R. W. Elner and R. L. Vadas, *Am. Nat.* **136**, 108 (1990).
6. M. J. Tegner and P. K. Dayton, *Mar. Ecol. Prog. Ser.* **77**, 49 (1991).
7. A. A. Berryman, *Oikos* **62**, 106 (1991).
8. L. W. Botsford *et al.*, *Top. Stud. Oceanogr.*, in press.
9. G. E. Hutchinson, *Am. Nat.* **95**, 137 (1961).
10. P. Barbosa and J. C. Shultz, Eds., *Insect Outbreaks* (Academic Press, San Diego, CA, 1987).
11. H. N. Comins, M. P. Hassell, R. M. May, *J. Anim. Ecol.* **61**, 735 (1992).
12. A. Hastings, *Ecology* **74**, 1362 (1993).
13. M. Kot and W. M. Schaffer, *Math. Biosci.* **80**, 109 (1986).
14. K. Kaneko, *Chaos* **2**, 279 (1992).
15. J. P. Crutchfield and K. Kaneko, *Phys. Rev. Lett.* **60**, 2715 (1988).
16. R. Livi, G. Martínez-Mekler, S. Ruffo, *Phys. D.* **45**, 452 (1990).
17. R. V. Solé, J. Bascompte, J. Valls, *Chaos* **2**, 387 (1992).
18. W. E. Ricker, *Can. Fish. Res. Board J.* **11**, 559 (1954).
19. For example, we obtained similar results with the logistic formulation $I(t,x) = rN(t,x)[1 - N(t,x)]$, where we modified dispersal so that the maximum number of individuals at any point is one.
20. We usually chose D to be between 400 and 800, but we obtained similar results for D between 40 and 4000.
21. J. Roughgarden, Y. Iwasa, C. Baxter, *Ecology* **66**, 54 (1985).
22. R. M. May, *Proc. R. Soc. London Ser. B* **228**, 241 (1986).
23. M. P. Hassell, *J. Anim. Ecol.* **56**, 705 (1987).
24. _____, T. R. E. Southwood, P. M. Reader, *ibid.*, p. 283.

25. We thank L. Botsford, E. Fingerett, S. Levin, and T. Powell for comments. Supported by grants from the Department of Energy and the National Science Foundation (BIR-9214381 and OCE-90-16721).

6 October 1993; accepted 7 January 1994

Sequential Interactions of the TCR with Two Distinct Cytoplasmic Tyrosine Kinases

Makio Iwashima, Bryan A. Irving, Nicolai S. C. van Oers, Andrew C. Chan,* Arthur Weiss†

The T cell antigen receptor (TCR) initiates signals by interacting with cytoplasmic protein tyrosine kinases (PTKs) through a 17-residue sequence motif [called the antigen recognition activation motif (ARAM)] that is contained in the TCRζ and CD3 chains. TCR stimulation induces the tyrosine phosphorylation of several cellular substrates, including the ARAMs. Lck kinase activity is required for phosphorylation of two conserved tyrosine residues in an ARAM. This phosphorylation leads to the recruitment of a second cytoplasmic PTK, ZAP-70, through both of the ZAP-70 Src homology 2 domains and its phosphorylation. Thus, TCR signal transduction is initiated by the sequential interaction of two PTKs with TCR ARAMs.

The multisubunit TCR is composed of the TCRαβ heterodimer, a ζ family homo- or heterodimer (ζ-ζ, ζ-η, or ζ-γ), and the CD3 chains (γ, δ, and ε) (*1*). With the use of chimeric receptors, the signal transduction functions of the TCR have been localized to a common motif, here called the ARAM, that contains the sequence $YXXLX_{(6-8)}$ YXXL (*2*) and is present in the cytoplasmic domains of ζ and each of the CD3 chains (*3–6*). One of the earliest events associated with TCR signal transduction is tyrosine phosphorylation of cellular proteins that include the ARAMs of the TCRζ and CD3 chains (*4, 5, 7*). Three PTKs have been implicated in TCR signal transduction: Lck, Fyn, and ZAP-70. Lck is not generally found directly associated with the TCR but interacts with the coreceptors CD4 and CD8, which colocalize with the TCR during antigen recognition (*8*). Studies of Lck-deficient cells indicate that Lck is essential for TCR signal transduction, including tyrosine phosphoprotein induction (*9, 10*). Fyn associates, albeit at low stoichiometry, with the TCRζ chain (*11*). Studies of Fyn-deficient mice reveal a TCR signal transduction defect in the most mature thymocyte subsets, but mature peripheral T cells are not as affected (*12*). After TCR stimulation, the cytoplasmic PTK ZAP-70 rapidly associates with the ζ and CD3 chains and undergoes tyrosine phosphorylation (*4, 13–15*). A 72-kD tyrosine phosphoprotein, presumably the related PTK Syk (*16*), associates with membrane immunoglobulin (Ig) on B cells and with the IgE Fc receptor on mast cells (*17*). Studies of chimeric transmembrane proteins that have included ZAP-70, Syk, Lck, or Fyn suggest that ZAP-70 or Syk can regulate the function of downstream signal transduction molecules (*18*).

The mechanism by which the TCR interacts with these distinct families of PTKs is not understood. Studies have shown that ZAP-70 associated only with tyrosine-phosphorylated ζ (*14*). In addition, the association of ZAP-70 with the CD8-ζ chimera in a COS cell that stably expresses a CD8-ζ chimera (COS-18) requires the co-expression of either Lck or Fyn with ZAP-70 (*14, 19*). In J.CaM1.6, a Jurkat-derived mutant line (*20*), TCR stimulation does not increase tyrosine phosphoproteins or activate the phosphatidylinositol pathway because of the loss of functional Lck (*10, 20*). TCR stimulation of Jurkat cells, but not of J.CaM1.6, resulted in ζ phosphorylation (Fig. 1A, upper panel) although both cells have equivalent amounts of ZAP-70, TCR, and ζ chain protein (Fig. 1B) (*20, 21*). Unlike Jurkat cells, neither a phosphorylated nor an unphosphorylated form of ZAP-70 associated with ζ in TCR-stimulated J.CaM1.6 cells (Fig. 1A, upper and lower panels, respectively). These results provide genetic evidence that Lck function is required for tyrosine phosphorylation of ζ and for the recruitment and tyrosine phosphorylation of ZAP-70.

The requirement for Lck was further analyzed in COS-18 cells. As we have already shown (*14, 19*), cotransfection of Lck with ZAP-70 results in the association of ZAP-70 with CD8-ζ, as well as in the tyrosine phosphorylation of ZAP-70 and CD8-ζ (Fig. 2). However, a kinase-inac-

Howard Hughes Medical Institute, Departments of Medicine and of Microbiology and Immunology, University of California, San Francisco, CA 94143, USA.

*Present address: Howard Hughes Medical Institute, Department of Medicine and Pathology, Washington University School of Medicine, St. Louis, MO 63110, USA.

†To whom correspondence should be addressed.